α-TRICALCIUM PHOSPHATE- AND TETRACALCIUM PHOSPHATE/DICALCIUM PHOSPHATE-BASED DUAL SETTING CEMENTS

E.C.S. RIGO[†], L.A. DOS SANTOS[‡], L.C.O. VERCIK[††], R.G. CARRODEGUAS[‡‡] and A.O. BOSCHI[†††]

[†] *Post-graduate Program in Engineering and Materials Science, University of São Francisco, 13251-900 Itatiba, SP, Brazil. eliana.rigo@saofrancisco.edu.br*

[‡] *Lab. of Biomaterials, Dept. of Materials, Federal University of Rio Grande do Sul (UFRGS), 91501-970 Porto Alegre, RS, Brazil. luis.santos@ufrgs.br*

[††] *Nuclear and Energetic Research Institute (IPEN), National Commission of Nuclear Energy, 05508-900 São Paulo, SP, Brazil. luciver cik@hotmail.com*

[‡‡] *Center of Biomaterials, University of Havana, 10600 La Habana, Cuba. rgc@biomat.uh.cu*

[†††] *Dept. of Materials Engineering (DEMa), Federal University of São Carlos (UFSCar), 13565-905 São Carlos, SP, Brazil. daob@power.ufscar.br*

***Abstract*— "Dual-setting" calcium phosphate cements (DS-CPCs), characterized by a polymerization reaction that proceeds along with the conventional hydraulic setting, were prepared and studied. Acrylamide (AA), 2-hydroxyethyl methacrylate (HEMA), and N-vinyl-2-pyrrolydone (VP) in 5, 10, and 20 wt./vol.-% were added to the liquid of α-tricalcium phosphate (α-TCP) and tetracalcium phosphate/dicalcium phosphate anhydrous (TTCP/DCPA) conventional cements. N,N'-methylenebisacrylamide was used as cross linking agent. N,N,N´,N´-tetramethylethylendiamine in the liquid, and ammonium persulfate in the powder, were employed as polymerization catalyst and initiator, respectively. Diametral tensile strength (DTS), setting time, phase composition, conversion rate, and microstructure of the DS-CPC were compared with those of non-added cements. The DTS increased 22 % for α-TCP and 85 % for TTCP/DCPA DS-CPCs by adding 20 wt./vol.-% AA. The HEMA and VP had no positive effect on DTS. The extent of the hydraulic setting reaction for α-TCP DS-CPC was only slightly decreased by the addition of 20 wt./vol.-% of AA to the mixing liquid.**

***Keywords*— calcium phosphate cement, dual-setting, α-tricalcium phosphate, tetracalcium phosphate, hydroxyapatite.**

I. INTRODUCTION

Calcium phosphate cements (CPC) are very promising materials for dental, orthopedic, and maxillo-facial applications because of their excellent biocompatibility and injectability. CPC based on α-$Ca_3(PO_4)_2$ (α-TCP) sets as the result of the precipitation of an entanglement of apatite crystals according to Eq. 1 (Driessens *et al.*, 1993).

$$3\alpha\text{-}Ca_3(PO_4)_2+H_2O\rightarrow Ca_9(HPO_4)(PO_4)_5OH \quad (1)$$

The resulting apatite is similar to bone mineral, and has excellent biocompatibility, bioactivity and osteointegrability (Driessens *et al.*, 1997).

However, the low strength of α-TCP CPC, especially shortly after initial setting, is a handicap that restricts its clinical applications (Ginebra *et al.*, 1997).

On the other hand, a water-soluble "in situ" polymerizing system based on acrylamide (AA), N,N'-methylenebisacrylamide (MBAA), ammonium persulfate (AP, initiator), and N,N,N',N'-tetramethylethylen-diamine (TEMED, accelerator) was first employed in gel-casting technology to bind together the particles of an aqueous slurry of ceramic powder. When polymerization is conducted a cross-linked polyacrylamide hydrogel is formed that binds and immobilizes the powder and provides with strength the resulting green body. Gel-casting technology has been successfully employed to manufacture hydroxyapatite ceramics (Padilla *et al.*, 2004).

In addition, the gel casting approach has been proposed to reinforce α-TCP-based CPC during the first stage of setting (García Carrodeguas *et al.*, 1999; Santos *et al.*, 1999; Davidenko *et al.*, 2002). The polyacrylamide network formed in the so-called "dual-setting" CPC effectively reinforced the material and is non toxic; however, residual acrylamide monomer may be released from the polyacrylamide hydrogel. Neurotoxic effects in humans, and carcinogenicity and reproductive disorders in rodents have been associated to exposure to acrylamide monomer. Also, abnormal transformations in Sirian hamster embryo cells cultured in presence of this monomer have been observed (Park *et al.*, 2002).

The gel casting approach has not been used to modify and improve the short term strength of other than α-TCP CPC. However, tetracalcium phosphate/dicalcium phosphate anhydrous (TTCP/DCPA) CPC produces also apatite by setting according to Eq. 2 (Brown and Chow, 1983) and has been extensively studied *in vitro* and *in vivo* with remarkable results. It also has low strength during the first stages after initial setting (Chow *et al.*, 1994).

$$2Ca_4(PO_4)_2O+2CaHPO_4+H_2O\rightarrow Ca_{10}(PO_4)_6(OH)_2 \quad (2)$$

Accordingly, this work was aimed to evaluate other non toxic monomers, like 2-hydroxyethyl methacrylate

(HEMA) and N-vinyl-2-pyrrolidone (VP) along with AA, for the preparation of "dual-setting" α-TCP- and TTCP/DCPA-based CPCs in order to increase their short term strength.

II. MATERIALS AND METHODS

A. Materials

For obtaining α-TCP, an appropriate mixture of γ-$Ca_2P_2O_7$ (prepared by dehydrating $CaHPO_4.2H_2O$ (IQUIMM, batch No. 1050498) at 550 °C for 2 h) and $CaCO_3$ (Labsynth, Cat. No. CI.006) was heated for 15 h at 1300 °C and quenched in air. After wet milling (anhydrous isopropanol, ball mill) for 2 h, its average particle size was 3.87 μm and contained 8.4 wt-% β-TCP and 5.0 wt.-% hydroxyapatite (HA). TTCP ($Ca_4(PO_4)_2O$) was prepared by heating a stoichiometric mixture of $CaCO_3$ and $CaHPO_4$ for 24 h at 1500 °, then cooling to 1300° in 0.5 h and quenching in air. After wet milling (isopropanol, ball mill) for 2 h the resulting TTCP had an average particle size of 1.93 μm and contained 14.0 wt-% HA. DCPA ($CaHPO_4$) was obtained drying $CaHPO_4.2H_2O$ overnight at 120 ° and dry milling (ball mill) for 24 h. Its average particle size was 1.81 μm and no crystalline impurities were detected. Precipitated hydroxyapatite (PHA) was synthesized by neutralizing 2.5 L of a 0.5 $mol.L^{-1}$ slurry of $Ca(OH)_2$ (Merck Cat. No. 102047) in the presence of 20 mL of 25 wt.-% NH_3 with 2.5 L of H_3PO_4 0.3 $mol.L^{-1}$ at 95 °C. Acid was added at a rate of 1 $L.h^{-1}$ with stirring. The precipitate was aged under stirring at 95 °C for 24 h, and then vacuum filtered, washed with water and ethanol, and dried at 110 °C overnight.

The monomers employed were AA (BDH, Cat. No. 27045), HEMA (Fluka Cat. No. 64170), VP (Riedel-de Haën, Cat. No. 63180), and MBAA (Fluka, Cat. No. 66670). AA and MBAA were used as received and HEMA and VP were vacuum distilled previously. The catalyst and initiator were TEMED (Aldrich, Cat. No. T2,250-0,) and AP (Aldrich, Cat. No. 24,861-4), respectively.

Simulated Body Fluid (SBF) was prepared as described elsewhere (Kokubo and Takadama, 2006).

The cement compositions considered are shown in Table 1. Formulations A and T in that table were previously developed and studied by Driessens *et al.* (1993) and Chow *et al.* (1994), respectively.

B. Methods

Samples preparation: Portions of 10 g of powder and the required amount of liquid were mixed with a spatula in a 100-mL beaker for about 1 min. The paste thus obtained was packed into the holes of a silicone mold which had a diameter of 20 mm and a height of 10 mm. The samples in the mold were maintained for 1 h at 100 % relative humidity (R. H.) and room temperature (27±1 °C). Cylinders of cement were removed from the mold and immersed in SBF at 37 °C for 1 and 7 days. For each period, 5 samples were prepared.

Diametral tensile strength: After removing from SBF, the samples were immediately tested for diametral tensile strength (DTS.) in a Universal Testing Machine Instron 5569 at a displacement rate of 1 mm/min. The pieces remaining from the DTS test were immersed in acetone to stop the hydraulic reaction and dried in air.

Setting time: Initial (I) and final (F) setting times were measured using the Gillmore needles (ASTM, 2000). A ring with a diameter of 20 mm and a height of

Table 1. Cement compositions

α-TCP CEMENTS	POWDER				LIQUID			L/P
	α-TCP (wt.-%)	PHA (wt.-%)	AP (wt.-%)	Na_2HPO_4 (wt./vol.-%)	MONOMER (wt./vol.-%)	MBAA (wt./vol.-%)	TEMED (wt./vol.-%)	(mL/g)
A	98.00	2.00	-	2.5	-	-	-	0.37
A-AA5	97.95	2.00	0.05	2.5	5.0 AA	0.1	0.156	0.37
A-AA10	97.95	2.00	0.05	2.5	10.0 AA	0.2	0.156	0.37
A-AA20	97.95	2.00	0.05	2.5	20.0 AA	0.4	0.156	0.37
A-HEMA5	97.95	2.00	0.05	2.5	5.0 HEMA	0.1	0.156	0.37
A-HEMA10	97.95	2.00	0.05	2.5	10.0 HEMA	0.2	0.156	0.37
A-HEMA20	97.95	2.00	0.05	2.5	20.0 HEMA	0.4	0.156	0.37
A-VP5	97.95	2.00	0.05	2.5	5.0 VP	0.1	0.156	0.37
A-VP10	97.95	2.00	0.05	2.5	10.0 VP	0.2	0.156	0.37
A-VP20	97.95	2.00	0.05	2.5	20.0 VP	0.4	0.156	0.37
TTCP/DCPA CEMENTS	POWDER				LIQUID			L/P
	TTCP (wt.-%)	DCPA (wt.-%)	AP (wt.-%)	NaH_2PO_4 ($mol.L^{-1}$)	MONOMER (wt./vol.-%)	MBAA (wt./vol.-%)	TEMED (wt./vol.-%)	(mL/g)
T	72.91	27.09	-	2.5	-	-	-	0.40
T-AA5	72.88	27.085	0.035	2.5	5.0 AA	0.1	0.156	0.40
T-AA10	72.88	27.085	0.035	2.5	10.0 AA	0.2	0.156	0.40
T-AA20	72.88	27.085	0.035	2.5	20.0 AA	0.4	0.156	0.40
T-HEMA5	72.88	27.085	0.035	2.5	5.0 HEMA	0.1	0.156	0.40
T-HEMA10	72.88	27.085	0.035	2.5	10.0 HEMA	0.2	0.156	0.40
T-HEMA20	72.88	27.085	0.035	2.5	20.0 HEMA	0.4	0.156	0.40
T-VP5	72.88	27.085	0.035	2.5	5.0 VP	0.1	0.156	0.40
T-VP10	72.88	27.085	0.035	2.5	10.0 VP	0.2	0.156	0.40
T-VP20	72.88	27.085	0.035	2.5	20.0 VP	0.4	0.156	0.40

10 mm was used as mold. All measurements were performed at room temperature. Three replicas of each cement formulation were tested.

Porosity: The dried pieces remaining from the DTS test were employed for porosity measurements by the Archimedes method in kerosene. Three replicas were used for each formulation.

X-ray diffraction: Powder X-ray diffraction patterns were recorded in a computer-controlled diffractometer Siemens D5000, employing Ni-filtered Cu K_α radiation. For qualitative analysis the dried pieces remaining from DTS test were milled under 70 μm and examined in continuous mode at 2°.min^{-1}.

Conversion of α-TCP in α-TCP-based cements was determined as follows: Two recently prepared samples were maintained at 27±1 °C and 100 % R.H. for the required period of time, at the end of which the samples were removed, crushed and immersed in acetone to stop the hydraulic setting reaction. After drying in air, the pieces were milled under 70 μm, and the X-ray diffraction patterns were obtained (22-30 and 47.5-51.5 °(2θ); 0.02 °(2θ) of step; 10 s of collecting time). The extent of conversion was calculated by means of Eq. 3

$$\text{Conv.} = [(I_0/I_s)-(I_t/I_s)]/[(I_0/I_s)-(I_\infty/I_s)] \quad (3)$$

where I_0, I_t and I_∞ represent the integrated intensity of the peaks corresponding to the converted phase, at the beginning, at time t, and at infinite time, respectively. I_s is the integrated intensity of the peak corresponding to the internal standard.

Table 2 displays the selected peaks for each phase. β-TCP, present in α-TCP as impurity, was used as internal standard as proposed by Ginebra *et al.* (1997). The selected peaks were scanned twice for each sample, and the obtained peak integrated intensities were averaged. Conversion was calculated from HA and α-TCP intensities and the average were reported.

Scanning electron microscopy: Microstructures of the cements were investigated on gold-coated fracture surfaces of the dried pieces remaining from DTS test. A Philips XL30 TMP D6615 scanning electron microscope was used.

Acid solubility and infrared spectra of the residues: Dried pieces remaining from the 24 h DTS test were digested in diluted HCl (1:4). The residue was washed with distilled water and dried in air. The infrared spectra of residues of dissolution were obtained in KBr pellets in a Fourier transform spectrometer ATI (Matson).

Statistical analysis: A Taguchi experimental design with a L_{18} orthogonal array was employed. The independent variables and their levels were Cement (A and T), Monomer (AA, HEMA, and VP), and Monomer Content (5, 10, and 20 wt./vol.-%). The results were processed with the software Statistica for Windows 5.0a.

Table 2. Selected peaks for α-TCP, HA y β-TCP.

Phase	2θ (°)	d (Å)	h k l	I/I_{100}
α-TCP	24,10	3,69	-2 6 1	33
HA	49,44	1,841	2 1 3	40
β-TCP	27,80	3,21	2 1 4	55

III. RESULTS AND DISCUSSION

A. Setting time

Table 3 shows initial and final setting times of the studied cement formulations.

The presence of 5, 10 and 20 wt./vol.-% of AA in the liquid and its polymerization "*in situ*" leaded to a reduction of the initial and final setting times for α-TCP-based cements. Appropriate values of I and F for clinical applications were obtained for the 20 wt./vol.-% AA level. On the other hand, HEMA and VP additions only produced significant shortening of the initial setting time for the 10 and 20 % levels and influence was not detected on the final setting time.

For TTCP/DCPA-based cements the addition of AA to the liquid at 5, 10 and 20 wt./vol.-% had not practical influence on the initial setting time. However, HEMA and VP provoked longer initial setting times. No influence on the final setting time was detected for any of the additives.

At the moment of mixing the AP present in the powder partially or totally dissolves and initiates the polymerization reaction of the monomers. Polymerization reactions are usually faster than the hydraulic setting reaction having place in calcium phosphate cements.

Thus, polymerization of monofunctional monomers in the presence of a minor amount of a bifunctional one yields a cross-linked polymeric network responsible for the initial hardening of the cement. The setting time results suggested that in α-TCP-based cements the polymerization rate grew in the order VP ≈ HEMA <AA.

The results of setting times for TTCP/DCPA-based cements indicated that the polymerization was inhibited or delayed, or the resulting cross-linked polymeric network was poorly developed in the first hour after mixing. Moreover, larger initial setting time in comparison to non-added cement (T) suggested that the conventional hydraulic setting reaction is disturbed by the presence of HEMA and VP and/or its polymers.

Table 3. Results of setting time and porosity.

CEMENT	S. T. (min)		P (s.d.) (%)	
	I	F	24 hr	7 days
A	19	>60	40 (2)	38 (2)
A-AA5	12	26	31 (2)	31 (1)
A-AA10	12	24	37 (1)	26 (1)
A-AA20	11	18	9 (1)	12 (1)
A-HEMA5	18	>60	35 (2)	33 (3)
A-HEMA10	15	>60	32 (2)	30 (4)
A-HEMA20	13	>60	27 (1)	30 (4)
A-VP5	20	>60	28 (7)	31 (1)
A-VP10	16	>60	31 (2)	34 (1)
A-VP20	15	>60	37 (2)	41 (4)
T	13	>60	41 (1)	31 (1)
T-AA5	12	>60	38 (2)	28 (3)
T-AA10	13	>60	37 (1)	34 (1)
T-AA20	15	>60	30 (1)	26 (1)
T-HEMA5	16	>60	39 (1)	36 (1)
T-HEMA10	20	>60	40 (1)	40 (1)
T-HEMA20	27	>60	36 (2)	33 (1)
T-VP5	18	>60	44 (1)	40 (1)
T-VP10	19	>60	43 (1)	42 (1)
T-VP20	25	>60	43 (1)	43 (1)

B. Diametral tensile strength

DTS strength values are shown in Figs. 1 and 2. The results of one-way classification ANOVA revealed that the addition of AA-, HEMA-, and VP-based "in situ" polymerization systems to α-TCP and TTCP/DCPA cements have significant effect for the two immersion periods in SBF ($p<0,05$).

After immersion for 24 h in SBF the average DTS of cements A-AA5 and A-AA10 were significantly greater ($p<0.05$) than the mean of non-added cement, A. DTS increased 41 and 39 % for A-AA5 and A-AA10, respectively. No significant difference was found between A-AA5 and A-AA10 for the same period. After immersion in SBF for 7 days only A-AA20 was significantly stronger than A, with an increase of 22 % in DTS.

For TTCP/DCPA CPCs, the addition of 10 and 20 % of the AA-based polymerization system had a significant positive effect on the strength for both periods of immersion.

The increase of DTS achieved by adding 20 wt./vol.-% AA to TTCP/DCPA cement was 58 % and 85 %, for 24 hr and 7 days immersion periods in SBF, respectively. The DTS reported for conventional TTCP/DCPA cement at the same L/P ratio used in this work was in the range of 5 MPa after 24 h of incubation at 100 % R.H. (Ishikawa and Asaoka, 1995). This value is lower than the DTS found in this work for T-AA20 after 24 h of immersion in SBF.

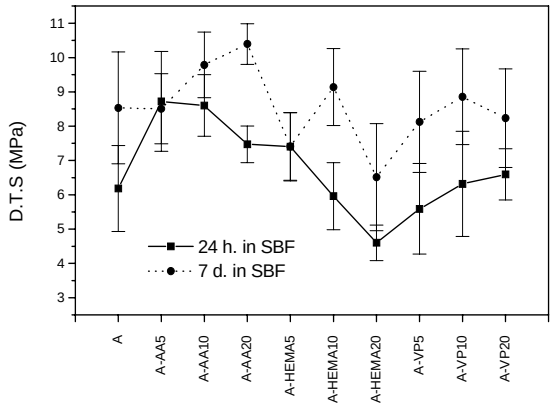

Fig. 1. Diametral tensile strength of α-TCP-based "dual-setting" cements.

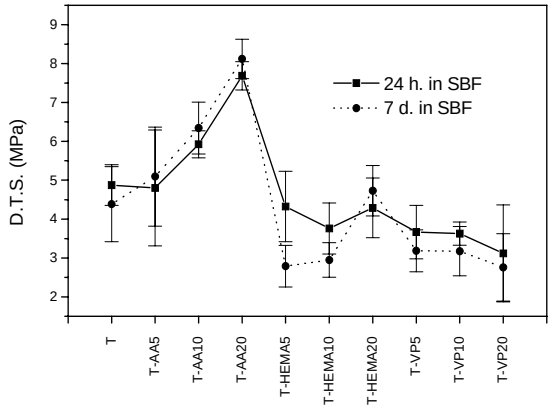

Fig. 2. Diametral tensile strength of TTCP/DCPA-based "dual-setting" cements.

As described in II.2., samples of A-AA20 and T-AA20 cements immersed for 24 h in SBF were leached with diluted HCl for 24 h at room temperature to dissolve the inorganic components. After the acid leaching, solid hydrogel masses were isolated which swelled to approximately twice its original volume. These polymeric masses did not disintegrate, keeping their original shape. This finding confirms the hypothesis of the reinforcement of the inorganic cement matrix by an interpenetrating network of cross linked polyacrylamide.

However, in "dual setting" cements prepared from the other monomers (A-HEMA20, A-VP20, T-HEMA20, and T-VP20) partial or almost total dissolution and disintegration of the organic matrix was observed indicating lower cross linking degree than in the case of A- and T-AA20.

The differences in solubility and cross linking observed could be caused by the differences in relative reactivity of the pairs of mono and bifunctional monomers employed, being the pair AA-MBAA the most effective were both monomers should exhibit similar reactivity for copolymerization. The other pairs of monomers (HEMA-MBAA and VP-MBAA) should present considerable differences in copolymerization reactivity, and homopolymerization is favored with regard to copolymerization, resulting in more soluble polymers with a lower degree of cross linking.

The infrared spectra of the insoluble residues matched those of the corresponding polymers: polyacrylamide for A- and T-AA20; poly(2-hydroxyethyl methacrylate) for A- and T-HEMA20, and poly(N-vinyl-2-pyrrolidone) for A- and T-VP20 (Hummel, 1978).

Typical load-deformation curves of A and A-AA20 cements are displayed in Fig. 3. The slopes (*m*) of the straight portions of the curves between 20 % and 80 % of the maximum load decreased as a consequence of the addition of AA.

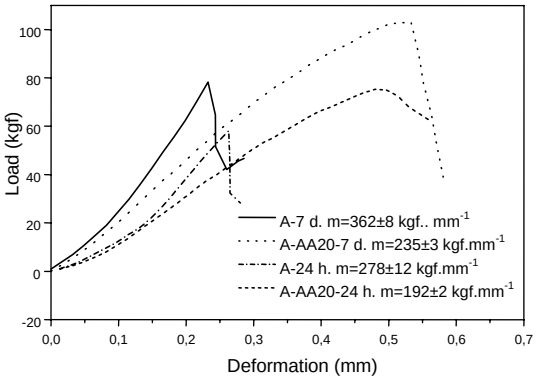

Fig. 3. Typical load-deformation curves for cements A and A-AA20. (m=slope of the portion of the curve between 20 and 80 % of maximum load).

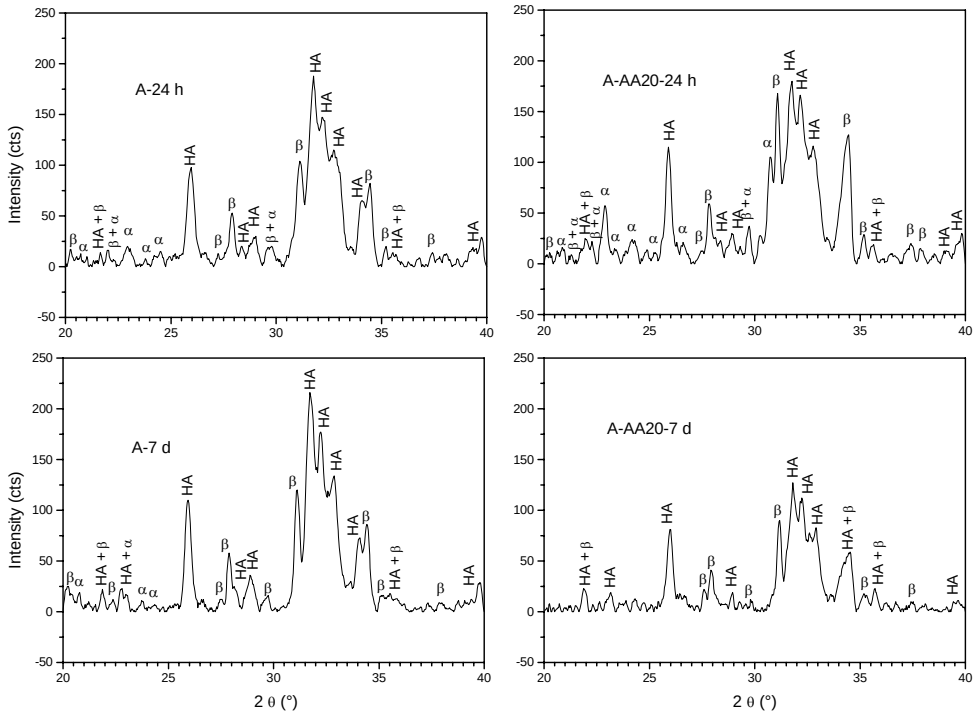

Fig. 4 X-ray diffraction patterns of cements A and A-AA20.

It could be said that Young's module (*E*), decreased by the addition of AA, since these slopes are directly related to *E*. A similar picture is observed for the other additives under study (HEMA, VP). Moreover, while in A and T cements a typical catastrophic fragile fracture is observed, in the cements containing 10 or 20 wt./vol.-% of additives in their liquids, the fragile behavior is substituted by a pseudoplastic one, admitting greater deflections and disappearing the catastrophic fracture.

This property could be interesting for certain clinical applications.

C. Porosity

Porosities of the studied cement formulations are listed in Table 3. The porosity values of the cements vary between 44 and 26 vol.-% except for the A-AA20 cement which has porosity values of 9 and 10 vol.-% at 24 hr and 7 days periods of immersion in SBF, respectively.

This lower porosity contributes to explain why the A-AA20 has the greater DTS.

D. X-ray diffraction

Figure 4 shows the X-ray diffraction pattern of cements A and A-AA20 after setting and immersion in SBF for 24 h and 7 days. The crystalline phases detected in both cements were HA (JCPDS 9-432), α-TCP (JCPDS 29-359) and β-TCP (JCPDS 9-169). The intensities of the α-TCP peaks at 22.2° (201) and 24.1° (161,-331) decreased when the time of immersion in SBF rose from 24 hr to 7 days, due to its transformation into HA.

The decrease was considerably higher for the cement A than for cement A-AA20. The I_0 peak of α-TCP was still perceptible in the diffraction pattern of A-AA20 after 24 h in SBF. The plot of conversion degree vs. time for cements A and A-AA20 is displayed in Fig. 5. The experimental points fitted very well the Eq. 4 proposed by Ginebra *et al.* (1997) for conventional α-TCP cement.

$$\text{Conv.} = 1 - \exp^{-kt} \qquad (4)$$

In the detail of Fig. 5 the plots of ln(1-Conv) versus t for A and A-AA20 cements are shown. Data fitted very well a straight line for both cements. The correlation coefficients obtained for the linear adjustment were 0.9973 and 0.9990 for A and A-AA20, respectively.

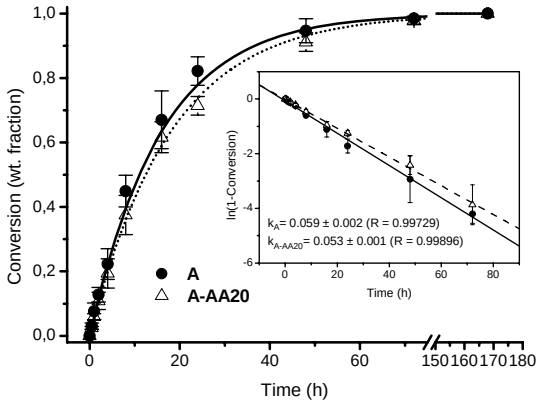

Fig. 5. Conversion degree of the hydraulic setting reaction as function of reaction time for cements A and A-AA20.

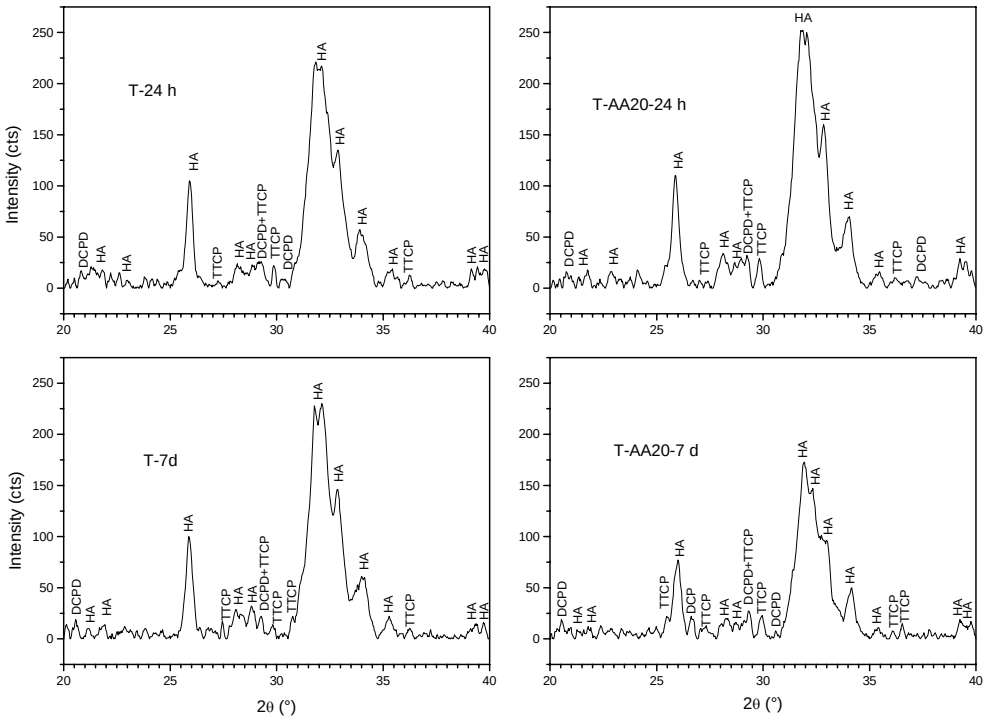

Fig. 6 X-ray diffraction patterns of cements T and T-AA20.

The *k* value of Eq. 4, calculated from the slope of the linear plots, were 0.059±0.002 and 0.053±0.001 h^{-1} for A and A-AA20, lower than the value found by Ginebra *et al.* (1997) for a conventional α-TCP CPC, for which they found a value of k=0.082±0.027 h^{-1}, possibly due to the higher temperature (37°C) employed by them during their experiment. The slightly lower value of k obtained for A-AA20 with regard to A, may be attributed to the presence of the AA gel, which acts as a diffusion barrier for the dissolution and precipitation processes that take place during the reaction of the Eq. 1 (Santos *et al.*, 1999; García Carrodeguas *et al.*, 1999).

For T and T-AA20 cements (Fig. 6) the crystalline phases detected were HA, TTCP (JCPDS 25-1137) and DCPD (JCPDS 9-77), the last one originated by hydration of the un-reacted DCPA. The peaks of TTCP and DCPA in T-AA20 were more intense than in T for both immersion periods, pointing to a minor conversion rate of the reaction represented by Eq. 2 in the cement modified with AA hydrogel. For T and T-AA20 the X-diffraction patterns did not vary significantly from 24 hr to 7 days immersion periods indicating that after 24 h in SBF the conversion of TTCP and DCPA into HA stopped.

A similar picture was observed for the cements modified with the other monomers under study.

E. Scanning Electron Microscopy

The SEM image of the microstructure of cement A after immersion in SBF for 7 days is displayed in Fig. 7a.

Small needle-like crystals of apatite were disposed around much bigger laminar apatite crystals. The small apatite crystals had radial or parallel orientations probably due to crystal growth (Ginebra *et al*., 1997).

The fracture was typically inter-crystalline.

The microstructure of cement A-AA20 (Fig. 7b) differed drastically. The small needle-like crystals were "embedded" in an amorphous matrix and laminar crystals were also observed. The microstructure was more compact than the one corresponding to the cement A (Fig. 7a).

Finally, A-VP20 showed almost the same characteristics in its fracture surface as the non-added cement A (Fig. 7d).

The micrographs of the fracture surfaces of the cements of the series T are displayed in Fig. 8.

No DCPD or TTCP unreacted particles were observed in any material.

In the micrograph corresponding to T-AA20 (Fig. 8b) an entanglement of acicular apatite crystals, which were smaller than those observed in the micrograph of cement A (Fig. 8a), was observed.

An amorphous substance over the surface was also noticed.

T-HEMA20 exhibited a similar structure but with even smaller apatite crystals (Fig. 8c) and the amorphous substance was also distinguishable.

However, the microstructure of T-VP20 (Fig. 8d) was very similar to that of the non-added cement T, being the size of apatite crystals the only difference noticed, which was smaller than in the non-added cement.

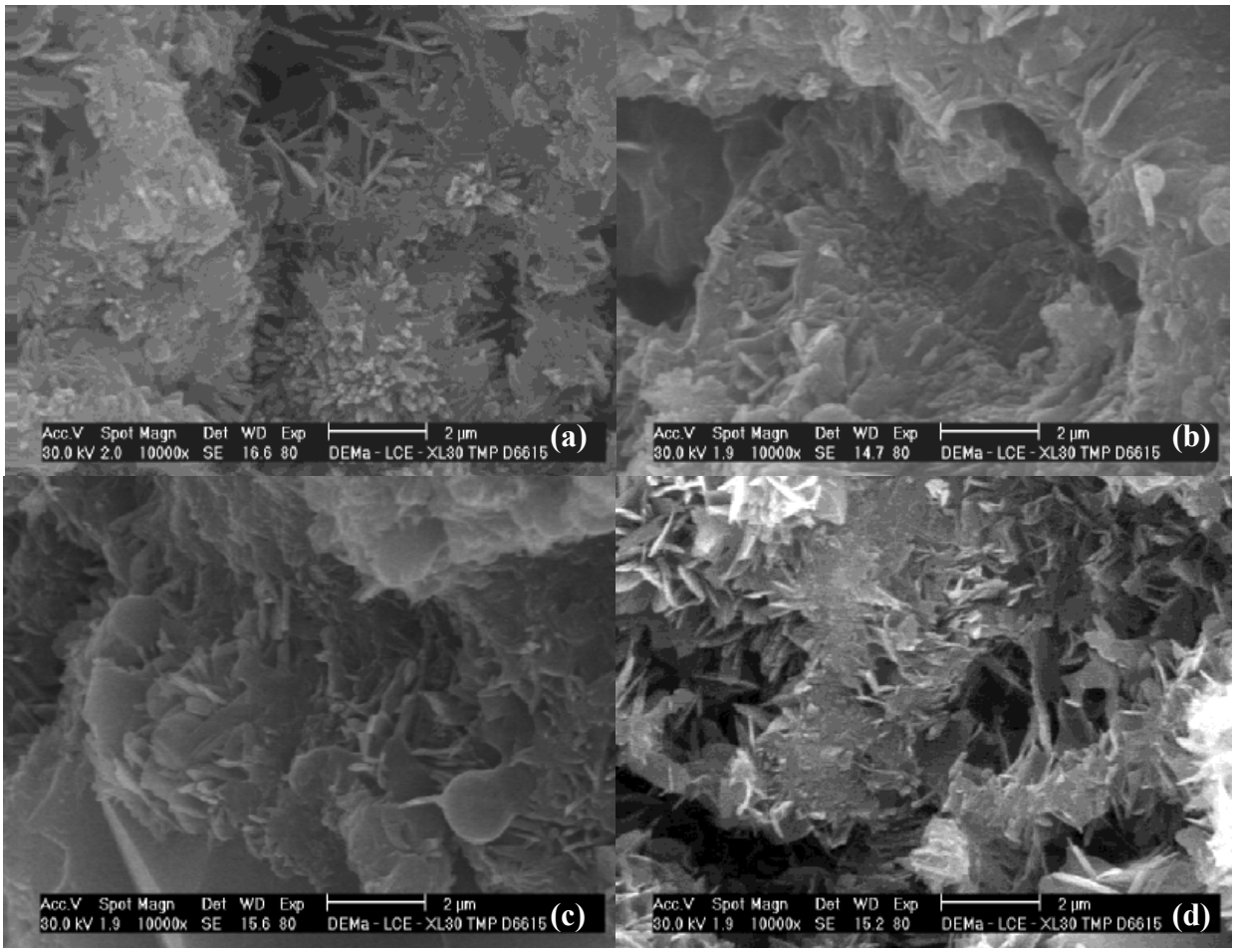

Fig. 7. Scanning electron micrographs of cements of A series after 7 days in SBF at 37°C. (a) A; (b) A-AA20; (c) A-HEMA20; (d) A-VP20.

The more compact microstructure, with the best crystalline entanglement corresponded to cements A, and A-AA20. In A-AA20 was clearly visible the AA hydrogel cementing the crystalline entanglement and providing the material with additional strength.

The polymer hydrogel was absent or scarcely developed in the other added cements.

These results are in agreement with the strength, porosity, solubility, and X-ray diffraction results previously exposed and discussed.

IV. CONCLUSIONS

The system of monomers consisting of AA/MBAA was the only effective to improve the properties of α-TCP- and TTCP/DCPA-based "dual-setting" CPCs. The improving effect was more remarkable in α-TCP- than in TTCP/DCPA-based "dual-setting" CPCs.

The main responsible for the increase in DTS in A-AA20 and T-AA20 was the cross-linked network of polyacrylamide hydrogel that reinforced the crystalline entanglement formed as a consequence of the hydraulic setting reactions, and decreased the total porosity of the material.

ACKNOWLEDGEMENTS

This study was supported by the Grants Nos. 98/11691-2, 98/00563-3, and 2006/52247-6 from FAPESP (Foundation for Research Support of the São Paulo State, Brazil).

R.G. Carrodeguas recognizes also the financial support received from the CYTED Network VIII.J "Biomaterials for Health".

REFERENCES

ASTM C266-99 "Standard Test Method for Time of Setting of Hydraulic Cement Paste by Gillmore Needles", *ASTM Book of Standards, Vol. 04-01: Cement, Lime, Gypsum*, ASTM, Philadelphia, (2000).

Brown, W.E. and L.C. Chow, "A new calcium phosphate setting cement", *J. Dent. Res.*, **62**, 672 (1983).

Chow, L.C., S. Takagi and K. Ishikawa, "Formation of hydroxyapatite in cement systems", in: Brown, P.W. and B. Constantz, editors *Hydroxyapatite and related materials*, CRC Press, Florida, 127-138 (1994).

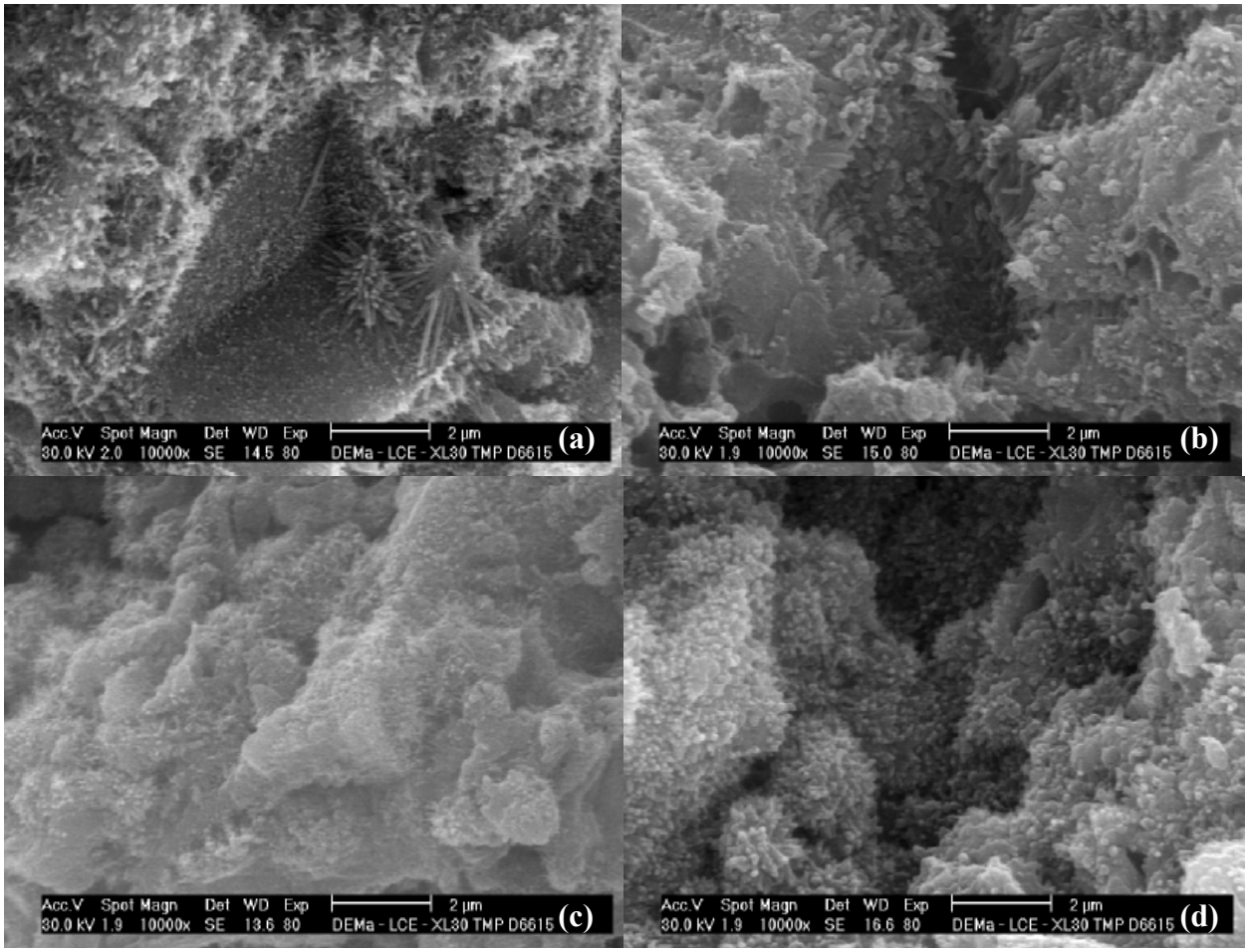

Fig. 8. Scanning electron micrographs of cements of T series after 7 days in SBF at 37°C. (a) T; (b) T-AA20; (c) T-HEMA20; (d) T-VP20.

Davidenko, N., R. García Carrodeguas, R. Sastre and J. San Román, "Photopolimerization of dual-setting α-tricalcium phosphate cements", *Int. J. Polymer. Mater.*, **51**, 577-589 (2002).

Driessens, F.C.M., M.G. Boltong, J.A. Planell, O. Bermúdez, M.P. Ginebra and E. Fernández, "A new apatitic calcium phosphate bone cement: Preliminary results", *Bioceramics (Proc. 6th Intl. Symp. Ceram. Med., Philadelphia, USA),* **6**, 469-473 (1993).

Driessens, F.C.M., E. Fernández, M.P. Ginebra, M.G. Boltong and J.A. Planell, "Calcium phosphates and ceramic bone cements vs. acrylic cements", *Anal. Quim. Int. Ed.,* **93**, S38-S43 (1997).

García Carrodeguas, R., L.A. Santos, L.C. Oliveira, E. Silva Rigo, A. Ortega Boschi and S. Padilla Mondéjar, "Cementos de α-fosfato tricálcico de fraguado doble", *Rev. CENIC. Ciencias Químicas*, **30**, 153-158 (1999).

Ginebra, M.P., E. Fernández, E.A.P. De Maeyer, R.M.H. Verbeeck, M.G. Boltong, J. Ginebra, F.C.M. Driessens and J.A. Planell, "Setting reaction and hardening of an apatitic calcium phosphate cement", *J. Dent. Res.*, **76** 905-912 (1997).

Hummel, D.O., *Atlas of Polymer and Plastic Analysis. Vol. I. Polymers Structure and Spectra,* 2nd Ed., VCH Publishers, Deerfield Beach, (1978).

Ishikawa, K. and K. Asaoka, "Estimation of the ideal mechanical strength and critical porosity of calcium phosphate cement", *J. Biomed. Mater. Res.*, **29**, 1537-1543 (1995).

Kokubo, T. and H. Takadama, "How useful is SBF in predicting in vivo bone bioactivity?", *Biomaterials*, **27**, 2907-2915 (2006).

Padilla, S., R. García Carrodeguas and M. Vallet-Regí, "Hydroxyapatite suspensions as precursors of pieces obtained by gelcasting method", *J. Eur. Ceram. Soc.*, **24**, 2223-2232 (2004).

Park, J., L.M. Kamendulis, M.A. Friedman and J.E. Klaunig, "Acrylamide-induced cellular transformation", *Toxicol. Sci.,* **65**, 177-183 (2002).

Santos, L.A., L.C. Oliveira, E.C.S. Rigo, R.G. Carrodeguas, A.O. Boschi and A.C.F. Arruda, "Influence of polymeric additives on the mechanical properties of α-tricalcium phosphate cements", *Bone*, **25**, 99S-102S (1999).

Received: August 30, 2006
Accepted: March 16, 2007
Recommended by Subject Editor: Orlando Alfano